Heredity (2016) 116, 52–59

www.nature.com/hdy

ORIGINAL ARTICLE

Mapping and recombination analysis of two moth colour mutations, Black moth and Wild wing spot, in the silkworm *Bombyx mori*

K Ito[1], S Katsuma[2], S Kuwazaki[3], A Jouraku[3], T Fujimoto[4], K Sahara[4], Y Yasukochi[3], K Yamamoto[3], H Tabunoki[1], T Yokoyama[1], K Kadono-Okuda[3] and T Shimada[2]

Many lepidopteran insects exhibit body colour variations, where the high phenotypic diversity observed in the wings and bodies of adults provides opportunities for studying adaptive morphological evolution. In the silkworm *Bombyx mori*, two genes responsible for moth colour mutation, *Bm* and *Ws*, have been mapped to 0.0 and 14.7 cM of the *B. mori* genetic linkage group 17; however, these genes have not been identified at the molecular level. We performed positional cloning of both genes to elucidate the molecular mechanisms that underlie the moth wing- and body-colour patterns in *B. mori*. We successfully narrowed down *Bm* and *Ws* to ~2-Mb-long and 100-kb-long regions on the same scaffold Bm_scaf33. Gene prediction analysis of this region identified 77 candidate genes in the *Bm* region, whereas there were no candidate genes in the *Ws* region. Fluorescence *in-situ* hybridisation analysis in *Bm* mutant detected chromosome inversion, which explains why there are no recombination in the corresponding region. The comparative genomic analysis demonstrated that the candidate regions of both genes shared synteny with a region associated with wing- and body-colour variations in other lepidopteran species including *Biston betularia* and *Heliconius* butterflies. These results suggest that the genes responsible for wing and body colour in *B. mori* may be associated with similar genes in other Lepidoptera.
Heredity (2016) **116,** 52–59; doi:10.1038/hdy.2015.69; published online 29 July 2015

INTRODUCTION

In Lepidoptera, adult body colour patterns are important for sexual selection, mimicry and predator avoidance (Parcham *et al.*, 2007). The wings of insects are believed to be a monophyletic adaptation that allowed the insects to exploit new niches, thereby resulting in rapid diversification. Many studies have investigated the factors that control the wing- and body-colour patterns of butterflies and moths; however, the underlying mechanism still remains unknown. Recently, the genomes and genomic information have been updated for various lepidopteran insects and molecular genetic studies have provided information that is useful for this field of study (International Silkworm Genome Consortium, 2008; Zhan *et al.*, 2011; Heliconius Genome Consortium, 2012; You *et al.*, 2013).

Over 50 body colour mutants have been reported in the silkworm *B. mori* (Banno *et al.*, 2010). However, most of these mutants correspond to larval body colour variations and few wing- and body-colour variations have been reported in this moth. Five mutants have been reported, that is, Black moth (*Bm*; Chikushi, 1960), black-striped pupal wing (*bpw*; Yamamoto, 1986), melanism (*mln*; Hasimoto, 1961), Wild wing spot (*Ws*; Doira *et al.*, 1981) and white-banded black wing (*wb*; Kanbe and Nara, 1959). Recently, the *mln* mutant, which exhibits a readily distinguishable phenotype in both the larvae and adults, was characterised at the molecular level based on positional cloning and functional analysis (Dai *et al.*, 2010; Zhan *et al.*, 2010). Linkage analysis and genomic studies have shown that *Bombyx arylalkamine-N-acetyl transferase*, the homologous gene (*Dat*) that converts dopamine into *N*-acetyl dopamine, encodes a precursor of *N*-acetyl dopamine, sclerotin in *Drosophila* and it is the gene responsible for *mln* (Dai *et al.*, 2010; Zhan *et al.*, 2010). However, other causal genes have not yet been identified.

The *Bm* mutant has black scales on the body and wings, which contrasts with the white appearance of the wild-type moth (Figure 1a). The gene responsible, *Bm*, has been mapped to 0.0 cM in *B. mori* genetic linkage group 17 (Chikushi, 1960) (Figure 1b). The *Ws* mutant strain exhibits a phenotype where the moth has a spot on the apex of its wing (Figure 1a). The *Ws* gene has been transferred by introgression from the wild silkworm *Bombyx mandarina*, which is widely believed to have the same ancestor as the domesticated silkworm *B. mori* (Goldsmith *et al.*, 2005). This gene has been mapped to 14.7 cM in linkage group 17 and it is linked to the *bts* (brown head and tail spot) gene (Doira *et al.*, 1981; Banno *et al.*, 2010) (Figure 1b). The *Bm* and *Ws* phenotypes are both dominant over the wild type. In addition, according to our observations these phenotypes are clearly exhibited in males, whereas it is difficult to distinguish mutant females from the

[1]Department of Science of Biological Production, Graduate School of Agriculture, Tokyo University of Agriculture and Technology, Fuchu, Tokyo, Japan; [2]Department of Agricultural and Environmental Biology, Graduate School of Agricultural and Life Sciences, The University of Tokyo, Bunkyo-ku, Tokyo, Japan; [3]Division of Insect Sciences, National Institute of Agrobiological Sciences, Tsukuba, Ibaraki, Japan and [4]Faculty of Agriculture, Iwate University, Morioka, Iwate, Japan
Correspondence: Dr K Ito, Department of Science of Biological Production, Tokyo University of Agriculture and Technology, 3-5-8 Saiwai-cho, Fuchu, Tokyo 183-8509, Japan.
E-mail: katsuito@cc.tuat.ac.jp
Received 20 April 2015; accepted 22 June 2015; published online 29 July 2015

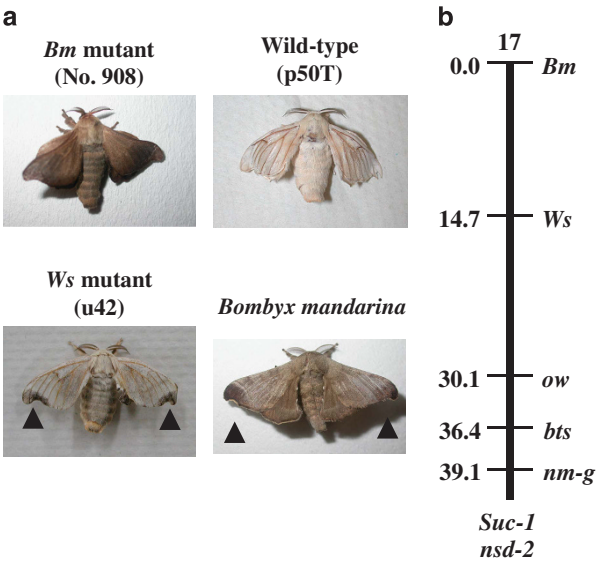

Figure 1 Phenotypes and linkage maps of the *Bm* and *Ws* mutations. (**a**) Phenotypes of *B. mori* wild type (p50T), *Bm* mutant (No. 908), *Ws* mutant (u42) and *B. manderina*. Arrowheads indicate the spot at the apex of the wing. (**b**) Linkage map of group 17. The loci are labelled based on their position in centimorgan units (left) and the locus name (right). Abbreviations: *Bm*, Black moth; *Ws*, Wild wing spot; *ow*, waxy translucent; *bts*, brown head and tail spot; *nm-g*, non-molting glossy; *nsd-2*, non-susceptibility to DNV-2; *Suc-1*, sucrase-1 (Banno *et al.*, 2010).

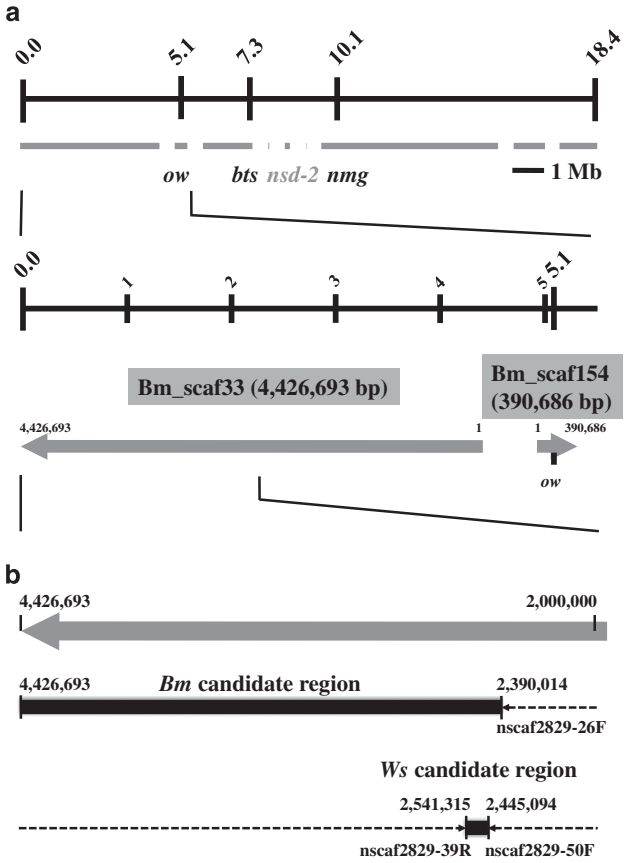

Figure 2 Mapping of the *Bm* and *Ws* mutations in linkage group 17. (**a**) Physical map and scaffold of linkage group 17. Black and grey lines indicate the physical map and the scaffold, respectively. The upper and lower figures indicate the whole and upstream regions of linkage group 17, respectively. The upper numbers indicate the positions that correspond to each gene (Ito *et al.*, 2008, 2009, 2010; Niwa *et al.*, 2010). *nsd-2* could not be mapped onto the physical map of group 17, because it was located on a non-mapped scaffold (Bm_scaf131). *ow* was mapped to the Bm_scaf154 (Ito *et al.*, 2009). (**b**) The narrowed down candidate region on the Bm_scaf33. The dotted arrows indicate the results of the detailed linkage analysis to narrow down the region linked to the *Bm* (upper) and *Ws* (lower) mutations (Table 2). The black boxes are candidate regions of each mutations.

wild type in BC_1 individuals. Recently, we succeeded in the positional cloning of four genes responsible for *bts*, *nm-g*, *nsd-2* and *ow*, which also map to linkage group 17 (Ito *et al.*, 2008, 2009, 2010; Niwa *et al.*, 2010) (Figures 1b and 2a). We consider that the genomic information obtained in previous studies may be a useful tool for isolating and identifying *Bm* and *Ws* mutations.

To better understand the molecular mechanisms that control colour variations in a Lepidoptera, we performed positional cloning and recombination analysis of two genes, that is, *Bm* and *Ws*. Based on mapping, we successfully narrowed down the candidate regions of both genes to one scaffold, Bm_scaf33. In addition, recombination analysis between *Bm* and *Ws*, and fluorescence *in-situ* hybridisation (FISH) analysis demonstrated that chromosome 17 carrying the *Bm* gene has inversion in the candidate region. Therefore, recombination between both genes occurred in none of the individuals. Moreover, we found that the candidate regions of both genes shared correspondence with a region associated with wing- and body-colour variations in different lepidopteran species, that is, *B. betularia*, *Heliconius cydno*, *Heliconius erato*, *Heliconius melpomene* and *Heliconius numata* (Joron *et al.*, 2006; Kronfost *et al.*, 2006; Papa *et al.*, 2008; Ferguson *et al.*, 2010; van't Hof *et al.*, 2011). These results strongly suggest that the same genes and/or regulatory elements responsible for wing and body colour in *Bombyx*, *Bm* and *Ws*, may underlie these variants in different Lepidoptera.

In this study, we demonstrate that the genomic context is highly relevant given the orthology in lepidopteran patterning regions and the fact that the *Ws* mutation appears to influence three nearby genes that do not fall within the 100-kb mapping interval. The apparent involvement of clustered genes in similar processes suggests the existence of a supergene. *B. mori* is the most advanced model Lepidoptera, thereby facilitating interpretation in a genomic context.

MATERIALS AND METHODS

Insects

The *Bm* (*Bm*/*Bm*; $+^{Ws}/+^{Ws}$) and the *Ws* ($+^{Bm}/+^{Bm}$; *Ws*/*Ws*) used No. 908 (National Institute of Agrobiological Sciences, Tsukuba, Japan) and u42 (Kyushu University, Fukuoka, Japan), respectively. The wild type ($+^{Bm}/+^{Bm}$; $+^{Ws}/+^{Ws}$) were p50T (University of Tokyo, Bunkyo-ku, Japan) and p50 (Kyushu University) (Figure 1a). BC_1 progeny from the cross p50T × (p50T × No. 908) and p50T × (p50T × u42) were used for mapping *Bm* and *Ws*, respectively. The offspring from the cross p50T × (u42 × No. 908) were used for the recombination analysis between *Bm* and *Ws*. All of the silkworm larvae were reared on mulberry leaves at 25 °C.

In the screening of BC_1, the *Bm* and *Ws* phenotypes present themselves clearly in males, while mutant females can be hard to distinguish from wild type. Therefore, we only used males in the analysis.

Preparation for genomic DNA and PCR analysis

DNA was isolated from moth legs using DNAzol (Invitrogen, Carlsbad, CA, USA) according to the manufacturer's protocol. PCR was performed using Ex Taq DNA Polymerase (Takara Bio, Otsu, Japan) and the primer sets are listed

in Supplementary Table S1. The PCR conditions were as follows: initial denaturation at 94 °C for 2 min followed by 35 cycles of denaturation at 94 °C for 15 s, annealing at 60 °C for 15 s and extension at 72 °C for 1 or 3 min with a final incubation step at 72 °C for 4 min.

Isolation of total RNA and reverse-transcriptase PCR analysis

Total RNA was isolated from the forewings of pupae and adults using TRIzol (Invitrogen) according to the manufacturer's protocol. The isolated RNA was reverse transcribed using an Oligo $(dT)_{12–18}$ primer (GE Healthcare, Buckinghamshire, UK) and Ready-to-Go RT-PCR Beads (GE Healthcare), according to the manufacturer's protocol, and the cDNA was then diluted 10-fold before reverse-transcriptase PCR (RT-PCR). RT-PCR was performed using Ex Taq DNA Polymerase, with the primer sets listed in Supplementary Table S1 in the following conditions: initial denaturation at 94 °C for 2 min followed by 30 cycles of denaturation at 94 °C for 15 s, annealing at 60 °C for 15 s and extension at 72 °C for 1 min followed by a final incubation at 72 °C for 4 min.

Positional cloning

Positional cloning of the *Bm* and *Ws* candidate genes was performed as previously described (Ito *et al.*, 2009). PCR and single-nucleotide polymorphism markers that exhibited polymorphism in the parents were detected at each position on chromosome 17. Mapping was performed using 1861 and 434 BC_1 progeny with the *Bm* and *Ws* phenotypes, respectively. Candidate genes in the region narrowed by linkage analysis were predicted and annotated using KAIKObase (http://sgp.dna.affrc.go.jp/KAIKObase/), KAIKOBLAST (http://kaikoblast.dna.affrc.go.jp/) and NCBI BLAST (http://blast.ncbi.nlm.nih.gov/Blast.cgi).

Recombination analysis between *Bm* and *Ws*

Recombination analysis was performed using 1163 male moths obtained by crossing wild-type females with F_1 males. The progeny could be classified according to four different phenotypes in terms of their body and wing colours: *Bm* type ($+^{Bm}/Bm$; $+^{Ws}/+^{Ws}$), *Ws* type ($+^{Bm}/+^{Bm}$; $+^{Ws}/Ws$), *Bm* and *Ws* type ($+^{Bm}/Bm$; $+^{Ws}/Ws$), and normal type ($+^{Bm}/+^{Bm}$; $+^{Ws}/+^{Ws}$) (Supplementary Figure S1). However, *Bm* is overdominant to *Ws* phenotype, which made it impossible to discriminate *Bm* and *Ws* type from *Bm* type. Hence, we count the former type together with the latter type. Recombination between *Bm* and *Ws* occurred in the *Bm* and *Ws* types and the normal type, but we judged only from the numbers of the normal type.

FISH analysis

Bacterial artificial chromosomes (BACs) used for FISH analysis were described by Yasukochi *et al.* (2006) (Table 1). We selected additional 4D3C and 3C11C BACs for the present study (Table 1). Chromosomes were prepared according to Sahara *et al.* (1999) and Yoshido *et al.* (2014). Briefly, female and/or male gonads were dissected from last instar larvae. The cells in the gonads were spread on a glass slide with 60% acetic acid at 50 °C. The chromosomes were air dried and stored until further use, at −20 °C after dehydration with an ethanol series of 70%, 80% and 99%. BAC-FISH analysis was performed as described by Yoshido *et al.* (2005) and Sahara *et al.* (2013). Briefly, BAC DNA extracted with a Plasmid Midi kit (Qiagen GmbH, Hilden, Germany) was labeled with fluorochromes (Orange-, Green- and Red-dUTP purchased from Abbott Molecular Inc., Des Plaines, IL, USA, and Cy5-dUTP from GE Healthcare) using a Nick Translation Mix (Roche Diagnostics Inc., Basel, Switzerland) (Table 1). Hybridisation was performed at 37 °C for 3 days, which was followed by washing with 0.1 × SSC and 0.1% Triton X-100. Re-probe technique was also used according to Shibata *et al.* (2009). The FISH preparations were counterstained and mounted with antifade (0.233 g 1,4-diazabicyclo(2.2.2)-octane, 1 ml 0.2 mM Tris-HCl, pH 8.0, 9 ml glycerol) containing 0.5 μg ml^{-1} DAPI (4′,6-diamidino-2-phenylindole; Sigma-Aldrich, St Louis, MO, USA). Signals were captured with a DFC350FX CCD camera mounted on a DM 6000B microscope (Leica Microsystems Japan, Tokyo, Japan) and processed with Adobe Photoshop CS6J (Adobe, San Jose, CA, USA).

Table 1 BAC probe information used for chromosome analysis and its primer sequences for the selection

BAC code	*Labeled dye*[a]	*Psuedo colour*	*Forward primer (5′–3′)*	*Reverse primer (5′–3′)*	*Product size (bp)*	*Position in KAIKObase*		
						Chromosomal	*Scaffold*	*Definition*
4D3C	O	Yellow	CAGGGTTCTTCTTTATTTTG	ATTGGCAGGTCAGTTCTCAT	572	chr17: 500 151–502 713	Bm_scaf33: 3 923 981–3 926 543	AY769310
5F11E	G	Cyan	GAAAACAAAACAAAAACAAT[b]	ACATCCAAAGAGTAAAGGTA[b]	755	chr17:1 490 552–1 489 034	Bm_scaf33: 2 936 142–2 937 660	B3L3G15[b]
1G10A	R	Red	CCGCAACTATCCACTACAT[b]	TAAGCAAATCTACTCACTC[b]	1139	chr17:1 688 344–1 687 205	Bm_scaf33: 2 739 386–2 741 910	AB019864[b]
3C11C	G	Green	TACCGTTGTATTCGCTTTA	ACAGTTGACTTTCTCCTTC	461	chr17: 2 177 038–2 178 320	Bm_scaf33: 2 248 374–2 249 656	DQ311300
1D2A	C5	Magenta	ACATAACTCAACGCAAAAGCA[b]	TGACTACGGACACTACCAAAC[b]	415	chr17:6 107 883–6 108 297	Bm_scaf92: 290504–290918	B16F2F32[b]

[a]O, G, R and C5 represent fluorochromes of Orange-dUTP, Green dUTP, Red-dUTP and Cy5-dUTP, respectively.
[b]See Yasukochi *et al.* (2006).

RESULTS

Mapping of *Bm* and *Ws*

To identify the genomic regions responsible for *Bm* and *Ws* mutations, we performed genetic linkage analysis referred by the *B. mori* single-nucleotide polymorphism linkage map (Yamamoto *et al.*, 2008) and genome sequence (International Silkworm Genome Consortium, 2008). The female body colour of BC_1 was too faint to allow us to distinguish each phenotype; therefore, we only used males for screening. We mapped the *Bm* mutation using ~1800 BC_1 individuals and narrowed down the *Bm*-linked region to between 2 390 014 (nscaf2829-26F) and 4 426 693 (the downstream terminal of the Bm_scaf33) (Figure 2 and Supplementary Table S2). This region was ~2-Mb long on the Bm_scaf33. Next, we performed gene prediction analysis for the candidate region using gene prediction models in KAIKOBLAST and we found 77 candidate genes (data not shown). For the *Ws* mutation, we delimited the locus to 100-kb-long regions between 2 445 094 (nscaf2829-50F) and 2 541 315 (nscaf2829-39R) on the Bm_scaf33 using ~400 BC_1 individuals (Figure 2 and Supplementary Table S2). However, there were no candidate genes within this region (data not shown). According to the linkage analysis of the *Bm* gene, although the mapping procedure used ~1800 BC_1 individuals, the *Bm*-linked region could not be narrowed down further within an ~2-Mb-long region on the Bm_scaf33, thereby suggesting suppression of recombination. Therefore, the *Bm*-narrowed region was wider than that of *Ws* (Figure 2).

Recombination analysis between *Bm* and *Ws*

To confirm the recombination between *Bm* and *Ws*, the moth phenotype was observed in seven egg batches obtained from the cross between wild type ($+^{Bm}/+^{Bm}$; $+^{Ws}/+^{Ws}$) females with F_1 males (*Bm* female × *Ws* male ($Bm/+^{Bm}$; $+^{Ws}/Ws$)) (Supplementary Figure S1 and Table 2). Among 1163 individuals obtained from 7 batches, none of the normal type expected as recombinants appeared (Table 2). The segregation ratio between *Bm* phenotype and *Ws* phenotype was ~1 : 1 (Table 2). These strongly suggested that recombination did not occur between *Bm* and *Ws* alleles (Table 2), although the genetic distance between both genes is 14.7 cM in the linkage map of *B. mori*.

FISH analysis

To confirm the possibility of suppression of crossing over, we performed FISH analysis of the pachytene nuclei of the wild type (p50) and *Bm* mutant (No. 908) using four BACs mapped on Bm_scaf33 and a BAC on Bm_scaf92. FISH analysis revealed that the five BAC probes mapped onto p50 in a sequence according to the KAIKObase information. However, the FISH signals between 4D3C (yellow) and 1G10A (red) were invertedly ordered in No. 908 (Figure 3 and Table 1). Therefore, a chromosomal inversion is apparent in No. 908. This chromosome feature explained why recombination was not observed between *Bm* and *Ws* loci.

Comparative genomic analysis of the *Bm* and *Ws* regions, and other lepidopteran genomes

Based on the comparative genomic analysis, we found that the *Bm* and *Ws* regions shared synteny with a region associated with wing- and body-colour variations in different lepidopteran species of *B. betularia* and *Heliconius* butterflies (Joron *et al.*, 2006; Kronfost *et al.*, 2006; Papa *et al.*, 2008; Ferguson *et al.*, 2010; van't Hof *et al.*, 2011). The *carbonaria* region, which determines the phenotype of industrial melanism in *B. betularia*, shared synteny with the upstream region of *B. mori* genetic linkage group 17, corresponding to 2 390 014–2 875 682 on the Bm_scaf33 (between *trehalase 1B* and *lrtp*) (Figure 4) (van't Hof *et al.*, 2011). This phenotype is very similar to the *Bm* phenotype. The *Ws* region shared synteny with *H. melpomene* linkage group 15 and this region was located between the *H. melpomene* yellow hindwing bar (*HmYb*) and *H. melpomene* hindwing margin (*HmSb*) candidate regions, corresponding to 2 880 220–2 568 710 and 2 195 440–2 281 515 on the Bm_scaf33, respectively (*HmYb*, between *BGIBMGA005665* and *005652*; *HmSb*, between *BGIBMGA005650* and *005559*) (Figure 4). Both of these causal genes determine wing colour variations in *H. melpomene* (Ferguson *et al.*, 2010). In addition, this region overlapped with the mimetic patterning regions, *Yb*, *P* and *Cr*, in other *Heliconius* species, that is, *H. cydno*, *H. erato* and *H. numata* (Joron *et al.*, 2006; Kronfost *et al.*, 2006; Papa *et al.*, 2008). These

Table 2 Segregation of moth phenotype in the cross normal (+/+, +/+) females × *Bm* and *Ws* (+/*Bm*, +/*Ws*) males

Batch numbers	*Moth phenotype*[a]		
	'Bm (+/Bm, +/+)' and 'Bm and Ws (+/Bm, +/Ws)'[b]	*'Ws (+/+, +/Ws)'*	*'Normal (+/+, +/+)'*
1	101	83	0
2	86	97	0
3	80	73	0
4	87	94	0
5	29	50	0
6	81	104	0
7	100	98	0

The female body colour was not clear and both phenotypes could not be distinguished.
[a]Only male was used for screening of the phenotypes.
[b]*Bm* (+/*Bm*, +/+) and *Bm*, and *Ws* (+/*Bm*, +/*Ws*) phenotypes could not be judged whether it was only *Bm* or *Bm* and Ws phenotype, because the majority of the phenotypes had black wings.

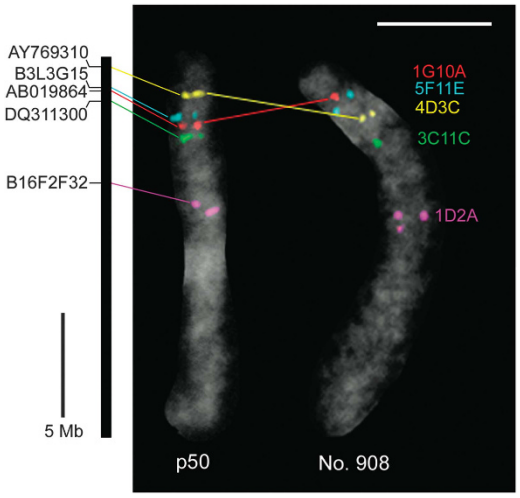

Figure 3 Inversion in chromosome 17 of *B. mori* No. 908 strain carrying the Black moth loci. The inverted order of FISH signals between 4D3C (yellow) and 1G10A (red) is apparent compared with the p50 strain. BAC codes are shown in the same colours as the signals. Marker sequence (see Yasukochi *et al.* 2006) or GenBank accession numbers for the BACs are shown on the left of the black bar, which represents *B. mori* chromosome 17 drawn to a relative scale in Mb taken from KAIKObase. White and black scale bars represent 5 μm and 5 Mb for the bivalents and chromosome 17, respectively. See Table 1 for details of the BAC probe information.

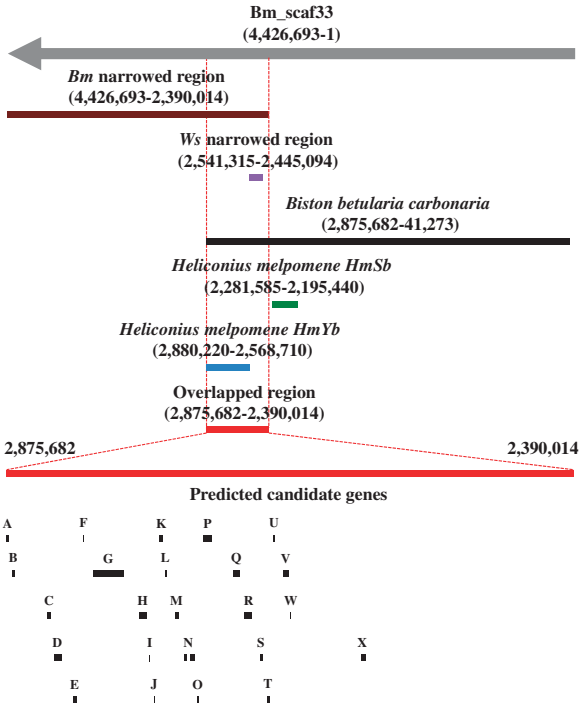

Figure 4 Localisation of *Bm* and *Ws* regions narrowed down to the Bm_scaf33 and their positional relationships with candidate regions of *carbonaria*, *HmSb* and *HmYb*. The brown, purple, black, blue and green bars indicate the *Bm*, *Ws*, *carbonaria*, *HmSb* and *Hmyb* regions, respectively. The red bar indicates the overlapping region for all genes. The *carbonaria* gene determines the phenotype of industrial melanism in the British peppered moth, *B. betularia* (van't Hof *et al.*, 2011). The *HmSb* and *HmYb* genes exhibit phenotypes with a hindwing margin and a yellow hindwing bar in *H. melpomene*, respectively (Ferguson *et al.*, 2010). Lower bars indicate 25 predicted genes. A, *BGIBMGA005665*; B, *005664*; C, *005663*; D, *005548*; E, *005662*; F, *005661*; G, *005549*; H, *005660*; I, *005550*; J, *005659*; K, *005551*; L, *005658*; M, *005552*; N, *005553* and *005554*; O, *005555*; P, *005556*; Q, *005657*; R, *005656*; S, *005557*; T, *005655*; U, *005558*; V, *005654*; W, *005653*; and X, *005652*. The letters correspond to Supplementary Figure S3 and Suppementary Table S3.

results suggest that this region may control wing- and body-colour variations in lepidopteran insects. Therefore, we focused on the predicted genes within the overlapping candidate regions of five genes, that is, *Bm*, *Ws*, *carbonaria*, *HmYb* and *HmSb* (Figure 4), and we performed gene expression analysis based on the RT-PCR results.

RT-PCR analysis of candidate genes in the overlapping region

Using KAIKObase, we predicted 24 *Bm* and *Ws* candidate genes within the overlapping region: *BGIBMGA005665* (A), *005664* (B), *005663* (C), *005548* (D), *005662* (E), *005661* (F), *005549* (G), *005660* (H), *005550* (I), *005659* (J), *005551* (K), *005658* (L), *005552* (M), *005553* and *005554* (N), *005555* (O), *005556* (P), *005657* (Q), *005656* (R), *005557* (S), *005655* (T), *005558* (U), *005654* (V), *005653* (W) and *005652* (X) (Figure 4 and Table 3). First, we investigated whether these candidate genes were expressed in the forewing from pupal day 0 to adult day 0 (Supplementary Figures S2 and S3). RT-PCR analysis demonstrated that seven candidate genes were expressed in the forewing, that is, *BGIBMGA005550* (I), *005658* (L), *005552* (M), *005657* (Q), *005656* (R), *005557* (S) and *005655* (T) (Supplementary Figure S3 and Table 3). In particular, three candidate genes, that is, *BGIBMGA005658* (L), *005657* (Q) and *005655* (T), exhibited clear differences in their expression profiles where these genes were properly expressed only in the wild-type strain (p50T) (Figure 5, Supplementary Figure S3 and Table 3). In the genomic PCR analysis using primer sets for these three differentially expressed genes, identical PCR products were obtained from respective genes in p50T, No. 908 and u42 individuals. These results suggest that the differences in the expression profiles were not due to the primer-binding sites but the expression levels (data not shown). Next, we cloned and sequenced four additional candidate genes, that us, *BGIBMGA005550* (I), *005552* (M), *005656* (R) and *005557* (S), and compared their sequences in the wild type (p50T), *Bm* mutant (No. 908) and *Ws* mutant (u42). According to the KAIKObase database search, these genes correspond to the full-length cDNA or expressed sequence tag clones AK383524; FS895121, FS917714 and FY019022; AK38029 and FY026966; and AK384540 and FY030309, respectively (Table 3). Therefore, we prepared primer sets based on the 5′- and 3′-untranslated regions using the sequences of each expressed sequence tag clone and performed RT-PCR analyses. Two candidate genes, that is, *BGIBMGA005550* (I) and *005656* (R), lacked mutations in the coding regions (Supplementary Figure S4) and we could not detect the transcripts of two candidate genes, *BGIBMGA005552* (M) and *005557* (S) (Supplementary Figure S4). Overall, the results of the PCR and sequencing analysis suggest that *BGIBMGA005658* (L), *005657* (Q) and *005655* (T) may be candidates for the *Bm* and *Ws* genes.

DISCUSSION

In this study, we attempted to isolate two genes responsible for moth colour mutations, that is, *Bm* and *Ws*, based on positional cloning using *B. mori* genome information. The genetic and genomic analysis demonstrated the following: (i) the candidate regions of the *Bm* and *Ws* genes are located in ~2-Mb-long and 100-kb-long regions on the same scaffold Bm_scaf33 of chromosome 17; (ii) chromosome 17 of *Bm* mutation harbours inversion within a compartment corresponding to Bm_scaf33; and (iii) the *Bm* and *Ws* regions share synteny with a region associated with wing- and body-colour variations in different lepidopteran species (Joron *et al.*, 2006; Kronfost *et al.*, 2006; Papa *et al.*, 2008; Ferguson *et al.*, 2010; van't Hof *et al.*, 2011). Based on our results, we hypothesise that this common region may control wing- and body-colour variations in lepidopteran insects. These results provide insights into the molecular mechanisms that control colour variations in Lepidoptera.

Chikushi (1960) mapped the *Bm* gene to 0.0 cM on *B. mori* genetic linkage group 17 based on three-point crosses using the *Bm*, *ow* and *bts* genes (Chikushi, 1960). In addition, Doira *et al.* (1981) reported that the *Ws* gene was located at 14.7 cM in the same linkage group based on recombination analysis between the *Ws* and *bts* genes. FISH analysis demonstrated that a proximal region of chromosome 17 in No. 908 has an inversion. Thus, no recombination among 1163 BC_1 individuals is most probably caused by suppression of chromosome crossing over. Taking into account for classical linkage analysis, similar pattern of gene expression results in the present study and recent finding for mimicry and pheromone response (Joron *et al.* 2011; Nishikawa *et al.* 2015; Wadsworth *et al.* 2015), inversion-associated mutation is a possible explanation for *Bm* origin. This supposes the *Bm* and *Ws* share a mechanism for regulating wing and body colouration. However, the classical recombination value was calculated by a combination of different cross-experiments (Chikushi, 1960, Doira *et al.* 1981). Hence, it is also possible to predict the *Bm* locates in the proximity to *Ws* as well as any position in ~2-Mb region in Bm_scaf33.

Table 3 Predicted genes on the overlapping region

No.[a]	*Predicted candidate gene*	*Size (bp)*	*Position on Bm_scaf33*	B. mori *EST*		*RT-PCR product*	*NCBI-blastp*
				Top hit EST name	*Tissue*		
A	BGIBMGA005665	1737	2 873 946–2 875 682	AK381626|fwgP06H20	Wing	△	Trehalase-like protein [*Heliconius erato*]
B	BGIBMGA005664	1740	2 868 742–2 870 481	AK384297|fcaL15008	Corpora allata	△	Trehalase precursor [*Bombyx mori*]
C	BGIBMGA005663	591	2 838 348–2 841 051	AK379306|ftes10022	Testis	×	Putative B9 protein [*Heliconius melpomene*]
D	BGIBMGA005548	594	2 829 200–2 835 667	E_FL_fufe_48N15_F_0|FS919927	Embryo	×	HM00008 [*Heliconius melpomene*]
E	BGIBMGA005662	1041	2 816 343–2 819 205	E_FL_ftes_50J04_R_0|FS903315	Testis	△	Putative WD40 repeat domain 85 [*Heliconius melpomene*]
F	BGIBMGA005661	351	2 809 822–2 810 172	AK382038|fdpe05B13	Diapause-destined embryo	×	Cyclin-dependent kinase 2 [*Biston betularia*]
G	BGIBMGA005549	2985	2 775983–2 802 234	No hit	—	×	Hypothetical protein KGM_17540 [*Danaus plexippus*]
H	BGIBMGA005660	1314	2 756 026–2 762 984	No hit	—	×	Putative unkempt [*Danaus plexippus*]
I	BGIBMGA005550	411	2 753 403–2 753 958	AK383524|MFB-10F15	Fat body	○	Histone H3 [*Actinoposthia beklemischevi*]
J	BGIBMGA005659	516	2 749 885–2 751 628	AK379353|ftes12C18	Testis	×	Hypothetical protein KGM_11305 [*Danaus plexippus*]
K	BGIBMGA005551	426	2 742 379–2 745 280	AK379178|ftes07B24	Testis	×	HM00016 [*Heliconius melpomene*]
L	**BGIBMGA005658**	**522**	**2 739 386–2 741 910**	**E_FL_ftes_35L07_F_0|FS886292**	**Testis**	○	**Gloverin 2 precursor [*Bombyx mori*]**
M	BGIBMGA005552	2406	2 729 127–2 732 029	FY019022|rbmov23p16	Ovary	○	Putative smooth muscle caldesmon [*Danaus plexippus*]
N	BGIBMGA005553	438	2 721 679–2 723 756	E_FL_fufe_16K04_F_0|FS909237	Embryo	×	Sorting nexin-8-like protein [*Heliconius erato*]
	BGIBMGA005554	576	2 715 598–2 719 407	No hit	—		Sorting nexin-8-like protein [*Heliconius erato*]
O	BGIBMGA005555	1521	2 711 826–2 713 346	No hit	—	×	Putative beta-fructofuranosidase [*Bombyx mori*]
P	BGIBMGA005556	879	2 700 631–2 708 135	E_FL_fwgP_39N15_F_0|FS93438	Wing	△	Glutaminyl-peptide cyclotransferase-like protein [*Heliconius erato*]
Q	**BGIBMGA005657**	**1389**	**2 676 659–2 682 113**	**AK387492|bmov26C16**	**Ovary**	○	**HM00021 [*Heliconius melpomene*]**
R	BGIBMGA005656	909	2 666 003–2 673 048	FY030309|bmte25h07	Testis	○	Enoyl-CoA hydratase precursor 1 [*Bombyx mori*]
S	BGIBMGA005557	531	2 657 185–2 659 641	FY026966|bmte16b06	Testis	○	ATP binding protein [*Bombyx mori*]
T	**BGIBMGA005655**	**1410**	**2 651 271–2 653 800**	**E_FL_ftes_26G19_R_0|FS897276**	**Testis**	○	**Leucine-rich repeat Protein soc-2-like protein [*Heliconius erato*]**
U	BGIBMGA005558	378	2 646 473–2 647 703	AK388012|bmte28L08	Testis	×	Putative ATP-binding protein [*Danaus plexippus*]
V	BGIBMGA005654	621	2 634 452–2 639 545	No hit	—	×	Hypothetical protein KGM_00352 [*Danaus plexippus*]
W	BGIBMGA005653	372	2 632 428–2 633 450	No hit	—	×	Hypothetical protein KGM_00351 [*Danaus plexippus*]
X	BGIBMGA005652	738	2 568 710–2 572 721	AK381234|fufe37G19	Embryo	×	Cell division cycle protein 20 [*Heliconius erato*]

Three candidate genes showed in bold font.
[a]The alphabets correspond to Figure 4 and Supplementary Figure S3.

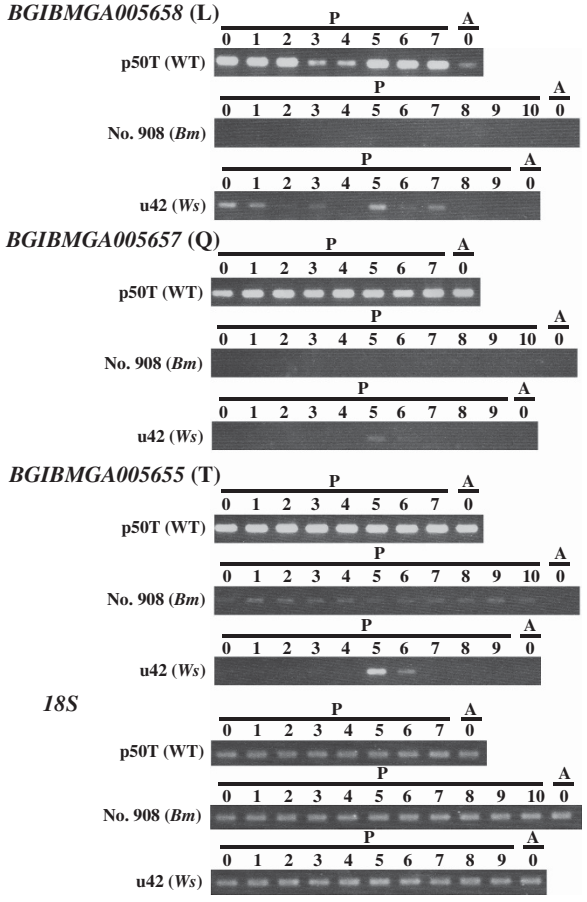

Figure 5 RT-PCR analysis of the candidate genes of *Bm* and *Ws*. Stage-specific expression profiles of three candidate genes, *BGIBMGA005658* (L), *005657* (Q) and *005655* (T), were investigated with p50T (wild type), No. 908 (*Bm* mutant) and u42 (*Ws* mutant) strains. P and A indicate pupa and adult, respectively. The numbers under the P and A bars show the day for each stage. *18S* ribosomal RNA was used as an internal control.

According to the linkage analysis of the *Ws* gene, we narrowed down *Ws* to a 100-kb-long region on the Bm_scaf33; however, there was no candidate gene within this region. Thus, the following two hypotheses are proposed. First, the nucleotide responsible for *Ws* mutation may correspond to a *cis*-regulatory element of *Ws*, which controls *Ws* expression in the spot at the apex of the wing. Second, the candidate gene may exist in an unknown genomic region that is specific to the mutant strain. This may explain why we could not find the candidate gene, because it was predicted using the genome sequence of the model strains p50T and Dazao, which exhibits the wild-type phenotype (International Silkworm Genome Consortium, 2008). Therefore, we are currently attempting to determine the genome sequence of the *Ws* mutant strain and *B. mandarina* by shotgun sequencing analysis.

RT-PCR analysis of the predicted genes indicated that three genes, that is, *BGIBMGA005658* (L), *005657* (Q) and *005655* (T), are current candidates for the *Bm* and *Ws* genes. The expression profiles of these genes revealed that transcripts were detected only in the wild-type strain (p50T), thereby suggesting that the phenotypes may be due to functional inactivation of these genes via haploinsufficiency or dominant-negative mutations. Investigations of the expression profiles of these genes using F_1 individuals will help to identify the gene responsible for these mutations. In addition, further gene expression analysis using RNA-seq and microarray will help to identify the genes responsible for *Bm* and *Ws*. Furthermore, *BGIBMGA005658* encodes the gloverin 2 precursor in *B. mori*; however, it is not present at the orthologous location in *Heliconius* (Ferguson *et al.*, 2010). This may be because of a difference in genome information between *Bombyx* and *Heliconius*. In general, gloverins have been reported to be antibacterial proteins in lepidopteran insects because of their antibacterial activity against *Escherichia coli*, Gram-positive bacteria, fungi and viruses (Kawaoka *et al.*, 2008; Yi *et al.*, 2013). Therefore, the possibility the gloverin 2 precursor is candidates for *Bm* and *Ws* genes will be a low.

The candidate regions of *Bm* and *Ws* genes shared synteny with a region associated with wing- and body-colour variations in different lepidopteran species (Joron *et al.*, 2006; Kronfost *et al.*, 2006; Papa *et al.*, 2008; Ferguson *et al.*, 2010; van't Hof *et al.*, 2011). The phenotypes of the *Bm* and *Ws* mutations comprise black scales on the moth body and a spot at the apex of wing, respectively. The colour of both mutants is mainly black; however, the coloured parts of the body differ from each other. In the *carbonaria* type of *B. betularia*, the phenotype has a black body colour, which is very similar to the *Bm* mutation. However, the *HmSb*, *HmYb*, *Cr*, *P* and *Yb* genes of *Heliconius* species are associated with mimetic patterning of the wings. The wing colouration is consistent with the phenotype of the *Ws* mutation. These results suggest that the control of colour pattern formation in lepidopterans may have a common genetic basis, although the critical factor has yet to be identified. Further studies to clarify the nature of this regulation will help to understand the molecular mechanisms that regulate the development of wing colouration.

Data archiving

The *B. mori* linkage maps and genetic markers used for genotyping are available from http://www.shigen.nig.ac.jp/silkwormbase/index.jsp and http://sgp.dna.affrc.go.jp/KAIKObase/.

CONFLICT OF INTEREST

The authors declare no conflict of interest.

ACKNOWLEDGEMENTS

We thank Mr Munetaka Kawamoto (University of Tokyo) for technical assistance and Dr Yutaka Banno (National BioResource Project (NBRP), Kyushu University) for providing the silkworm strains. This research was supported by grants from MAFF-NIAS (Agrigenome Research Program), MEXT (KAKENHI No. 22128004), NBRP (National BioResource Project) and JST (Professional Program for Agricultural Bioinformatics), Japan.

Banno Y, Yamamoto K, Nishikawa K, Tamura K, Yamamoto K, Aso Y (2010). Integration of the twenty-fourth and twenty-seventh linkage groups of the silkworm *Bombyx mori*. *J Insect Biotech Sericol* **79**: 67–70.

Chikushi H (1960). A new linkage group of the silkworm, *Bombyx mori*. *J Seric Sci Jpn* **29**: 278 in Japanese.

Dai FY, Qiao L, Tong XL, Cao C, Chen P, Chen J *et al.* (2010). Mutations of an arylalkylamine-*N*-acetyltransferase, *Bm-iAANAT*, are responsible for silkworm melanism mutant. *J Biol Chem* **285**: 19553–19560.

Diora H, Kihara H, Masuda S (1981). Linkage analysis of the 'Wild wing spot' gene in the silkworm. *Proc Sericult Sci Kyushu* **12**: 64 (in Japanese).

Ferguson L, Lee SF, Chamberlain N, Nadeau N, Joron M, Baxter S *et al.* (2010). Characterization of a hotspot for mimicry: assembly of a butterfly wing transcriptome to genomic sequence at the *HmYb/Sb* locus. *Mol Ecol* **19**: 240–254.

Goldsmith MR, Shimada T, Abe H (2005). The genetics and genomics of the silkworm *Bombyx mori*. *Annu Rev Entomol* **50**: 71–100.

Hasimoto H (1961). Genetika studo pri melanismo če morusa silkraŭpo, *Bombyx mori*. *J Seric Sci Jpn* **30**: 389 (in Japanese with Esperanto summary).

Heliconius Genome Consortium (2012). Butterfly genome reveals promiscuous exchange of mimicry adaptations among species. *Nature* **487**: 94–98.

International Silkworm Genome Consortium (2008). The genome of a lepidopteran model insect, the silkworm *Bombyx mori*. *Insect Biochem Mol Biol* **38**: 1036–1045.

Ito K, Katsuma S, Yamamoto K, Kadono-Okuda K, Mita K, Shimada T (2009). A 25 bp-long insertional mutation in the *BmVarp* gene causes the waxy translucent skin of the silkworm, *Bombyx mori*. *Insect Biochem Mol Biol* **39**: 287–293.

Ito K, Katsuma S, Yamamoto K, Kadono-Okuda K, Mita K, Shimada T (2010). Yellow-e determines the color pattern of larval head and tail spots of the silkworm *Bombyx mori*. *J Biol Chem* **285**: 5624–5629.

Ito K, Kidokoro K, Sezutsu H, Nohata J, Yamamoto K, Kobayashi I *et al.* (2008). Deletion of a gene encoding an amino acid transporter in the midgut membrane causes resistance to a *Bombyx* parvo-like virus. *Proc Natl Acad Sci USA* **105**: 7523–7527.

Joron M, Papa R, Beltrán M, Chamberlain N, Mavárez J, Baxter S *et al.* (2006). A conserved supergene locus controls color pattern diversity in *Heliconius* butterflies. *PLoS Biol* **4**: e303.

Joron M, Frezal L, Jones RT, Chamberlain NL, Lee SF, Haag CR *et al.* (2011). Chromosomal rearrangements maintain a polymorphic supergene controlling butterfly mimicry. *Nature* **477**: 203–206.

Kanbe R, Nara S (1959). Gemetical studies of a new mutamt, white bamded black (*wb*) wing, in silkworm. *J Seric Sci Jpn* **28**: 37 (in Japanese).

Kawaoka S, Katsuma S, Daimon T, Isono R, Omuro N, Mita K *et al.* (2008). Functional analysis of four Gloverin-like genes in the silkworm *Bombyx mori*. *Arch Insect Biochem Physiol* **67**: 87–96.

Kronforst MR, Kapan DD, Gilbert LE (2006). Parallel genetic architecture of parallel adaptive radiations in mimetic *Heliconius* butterflies. *Genetics* **174**: 535–539.

Nishikawa H, Iijima T, Kajitani R, Yamaguchi J, Ando T, Suzuki Y *et al.* (2015). A genetic mechanism for female-limited Batesian mimicry in *Papilio* butterfly. *Nat Genet* **47**: 405–409.

Niwa R, Namiki T, Ito K, Shimada-Niwa Y, Kiuchi M, Kawaoka S *et al.* (2010). *Non-molting glossy/shroud* encodes a short-chain dehydrogenase/reductase that functions in the 'Black Box' of the ecdysteroid biosynthesis pathway. *Development* **137**: 1991–1999.

Papa R, Morrison CM, Walters JR, Counterman BA, Chen R, Halder G *et al.* (2008). Highly conserved gene order and numerous novel repetitive elements in genomic regions linked to wing pattern variation in Heliconius butterflies. *BMC Genomics* **9**: 345.

Parchem RJ, Perry MW, Patel NH (2007). Patterns on the insect wing. *Curr Opin Genet Dev* **17**: 300–308.

Sahara K, Marec F, Traut W (1999). TTAGG telomeric repeats in chromosomes of some insects and other arthropods. *Chromosome Res* **7**: 449–460.

Sahara K, Yoshido A, Shibata F, Fujikawa-Kojima N, Okabe T, Tanaka-Okuyama M *et al.* (2013). FISH identification of *Helicoverpa armigera* and *Mamestra brassicae* chromosomes by BAC and fosmid probes. *Insect Biochem Mol Biol* **43**: 644–653.

Shibata F, Sahara K, Naito Y, Yasukochi Y (2009). Reprobing of multicolour FISH in preparations of lepidopteran chromosomes. *Zoolog Sci* **26**: 187–190.

van't Hof AE, Edmonds N, Dalíková M, Marec F, Saccheri IJ (2011). Industrial melanism in British peppered moths has a singular and recent mutational origin. *Science* **332**: 958–960.

Wadsworth CB, Li X, Dopman EB (2015). A recombination suppressor contributes to ecological speciation in *OSTRINIA* moths. *Hered Adv online* **114**: 593–600.

Yamamoto T (1986). Linkage group of the black-striped pupal wing gene in the silkworm. *Proc J Seric Sci Jpn* **56**: 60 (in Japanese).

Yamamoto K, Nohata J, Kadono-Okuda K, Narukawa J, Sasanuma M, Sasanuma S *et al.* (2008). A BAC-based integrated linkage map of the silkworm *Bobmyx mori*. *Genome Biol* **9**: R21.

Yasukochi Y, Ashakumary LA, Baba K, Yoshido A, Sahara K (2006). A second generation integrated map of the silkworm reveals synteny and conserved gene order between lepidopteran insects. *Genetics* **173**: 1319–1328.

Yoshido A, Bando H, Yasukochi Y, Sahara K (2005). The *Bombyx mori* karyotype and the assignment of linkage groups. *Genetics* **170**: 675–685.

Yoshido A, Sahara K, Yasukochi Y (2014). Chapter 6; Silkmoths (Lepidoptera). In: Sharakhov IV (ed). *Protocols for Cytogenetic Mapping of Arthropod Genomes*. CRC Press: London, pp 219–256.

You M, Yue Z, He W, Yang G, Xie M, Zhan D *et al.* (2013). A heterozygous moth genome provides insights into herbivory and detoxification. *Nat Genet* **45**: 220–225.

Yi HY, Deng XJ, Yang WY, Zhou CZ, Cao Y, Yu XQ (2013). Gloverins of the silkworm *Bombyx mori*: structural and binding properties and activities. *Insect Biochem Mol Biol* **43**: 612–625.

Zhan S, Guo Q, Li M, Li M, Li J, Miao X *et al.* (2010). Disruption of an N-acetyltransferase gene in the silkworm reveals a novel role in pigmentation. *Development* **137**: 4083–4090.

Zhan S, Merlin C, Boore JL, Reppert SM (2011). The monarch butterfly genome yields insights into long-distance migration. *Cell* **147**: 1171–1185.

Supplementary Information accompanies this paper on Heredity website (http://www.nature.com/hdy)